www.czasopisma.pan.pl PAN POLSKA AKADEMIA NAUK www.journals.pan.pl

A R C H I V E S O F M E T A L L U R G Y A N D M A T E R I A L S

Volume 59 2014 Issue 3

DOI: 10.2478/amm-2014-0145

R. BOGUCKI*, S.M. PYTEL*

# INFLUENCE OF MOLYBDENUM ADDITION ON MECHANICAL PROPERTIES OF LOW CARBON HSLA-100 STEEL

# WPŁYW DODATKU MOLIBDENU NA WŁASNOŚCI MECHANICZNE NISKOWĘGLOWEJ STALI HSLA-100

The results of mechanical properties and microstructure observation of low carbon copper bearing steel with high addition of molybdenum are presented in this paper. This steels were characterized by contents of molybdenum in the range from 1,02 to 2.94% wt. After the thermo -mechanical processing the steels were subsequently quenched and tempered in the temperature range from 500°C to 800°C for 1h. The changes of mechanical properties as function of tempering temperature were typical for the steel with the copper addition. The sudden drop of impact resistance after tempering from 575°C to 600°C was caused probably by precipitates of Laves phase of type $Fe_2Mo$.

*Keywords*: High Strength Low Alloyed steels (HSLA steels), effect of copper and molybdenum additions, microstructure, mechanical properties, heat treatment

W pracy przedstawiono wyniki badań własności mechanicznych oraz obserwacji mikroskopowych nisko węglowych stali z dodatkiem Cu o podwyższonej koncentracji molibdenu w zakresie od 1,02 do 2,94% wag. Po obróbce cieplno-plastycznej stale były hartowane i odpuszczane w zakresie temperatur od 500-800°C przez 1 godzinę. Przebieg zmian własności mechanicznych w funkcji temperatury odpuszczania był zbliżony do przebiegu stali z dodatkiem miedzi. Silny spadek udarności po odpuszczaniu od 575 do 600°C spowodowany był prawdopodobnie procesami wydzieleniowymi fazy Lavesa typu $Fe_2Mo$.

## 1. Introduction

Since the mid-80's the low carbon structural steels with copper addition have been primary group of materials applied for heavily loaded marine structures such as drilling platforms, shell plating of submarines, destroyers and aircraft carriers. This group includes two basic grades of the steels designated according to ASTM A710 standard as HSLA-80 and HSLA-100 [1-5]. In these steels, copper addition was used at the level of 1.0-1.7% wt. in order to limit the drop in strength due to a considerable reduction of carbon which content does not exceed 0.06% wt. This low content of carbon is required to improve the steel weldability. High mechanical properties are obtained as a result of strong refinement of microstructure after thermo-mechanical processing, strengthening of ε-Cu phase precipitations and low-temperature transformation products of austenite as well as high metallurgical quality of the steels [1,5-7]. Many experimental studies conducted on the steels with copper content revealed a characteristic pattern of changes which is a consequence of precipitation processes and the decomposition of the martensitic matrix [1-5]. Optimal combination of mechanical properties is due to obtain the microstructure composed of the polygonal ferrite phase with precipitates of ε-Cu and the newly martensite laths area formed from retained austenite [1,5,8]. Currently, further work on the development of this group of materials have been performed. Research is conducted in two directions. The first method is based on modification of the chemical composition, particularly by the increase of Cu and Mo concentration [9-15]. The second method consists in shaping of the microstructure during the thermo-mechanical processing [13,16-18]. The following paper presents the effect of the chemical composition modification by increasing the content of Mo in the range of 1.02-2.94% wt. on the mechanical properties of HSLA-100 steel.

## 2. Experimental procedure

The three laboratory heats were melted in an air induction furnace with a weight of 50 kg each. The analysis of the chemical composition of the heats was performed on spectrometer Q4TASMAN and the results are shown in Table 1. Analyzed heats characterized by increased content of Mo as compared to the conventional low carbon HSLA steel with the Cu addition.

The thermo-mechanical processing was performed as presented in Fig.1. In first stage of treatment the ingot was heated up to 1250°C and next rolling was carried out in temperature range from 1200 to 1100°C with total reduction of $\delta$ =25%. Then the slabs were cooled in air to ambient temperature. In the second stage a conventional controlled rolling was applied. The ingot was heated below recrystallization temperature of

* INSTITUTE OF MATERIALS SCIENCE, CRACOW UNIVERSITY OF TECHNOLOGY, AL. JANA PAWŁA II 37, 31-864 KRAKÓW, POLAND

austenite (up to 950°C) and rolled with reduction equal to $\delta$ =50%. As a result of rolling procedure plate with 25 mm thickness was obtained.

TABLE 1

Chemical composition of the steels tested (wt.%)

| Steel | C | Mn | Si | Ni | Mo | Cu | Ti | Al |
|---|---|---|---|---|---|---|---|---|
| W1 | 0,015 | 1,00 | 0,29 | 3,53 | 1,02 | 1,50 | 0,02 | 0,005 |
| W2 | 0,017 | 0,89 | 0,27 | 3,55 | 1,88 | 1,51 | 0,02 | 0,005 |
| W3 | 0,017 | 1,00 | 0,29 | 3,53 | 2,94 | 1,50 | 0,02 | 0,006 |

Other elements: P=0,005%, S=0,003%, Nb=0,05%

In order to determine a phase transformation temperature of the steels the measurement using dilatometer NETZSCH TASC 414/2 were carried out. The dilatometer analysis was conducted in argon atmosphere using cylindrical samples with 4 mm diameter and 25 mm length orientated transversely to rolling direction. The specimens were heated up to 950°C and then cooled at rate about 20°C/min.

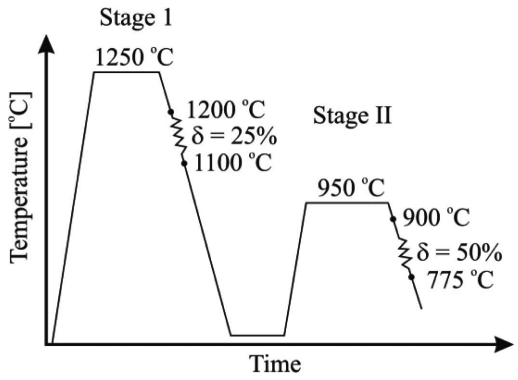


Fig. 1. Scheme of thermo- mechanical processing

The heat treatment of the steel consisted of austenitizing at 920°C for one hour and then quenching in water. Next samples were tempered in the temperature range from 500°C to 800°C for one hour (with step 25°C within), followed by quenching in water.

Hardness measurements were conducted in a Vicker's hardness tester under 30 kg in accordance with PN-EN ISO 6507-1:2006 E. Tensile test was performed in accordance with EN 10002-1:2001 at room temperature using the specimens prepared transversely to the rolling direction of the plate. For each tempering temperature three cylindrical specimens with 5 mm diameter and 25 mm gauge length were prepared. The test was carried out on the 20 EU hydraulic testing machine. Impact test was conducted by means of standard Charpy V-notch (CVN) specimens using impact testing hammer with initial energy of 300 J. The impact energy was determined at 25°C and -84°C (-120°F) temperature. Microstructure examinations of the tempered samples were conducted using NIKON ME 60 metallurgical microscope and JOEL JSM5510LV Scanning Electron Microscope (SEM). Observations were carried out on longitudinal sections of metallographic specimens etched in 4% nital. Stereological analysis of steels was performed using the software Aphelion 3.2.

A detailed assessment of microstructure for selected specimens characterized by the highest mechanical properties was carried out using Philips CM 20 Transmission Electron Microscopy (TEM). Thin foils were prepared at -50°C in a jet-polishing Struers TenuPol-5 using a 30% solution of nitric acid in ethanol. Identification of observed phases was carried out by indexed Selected Area Diffraction (SAD) pattern. Interplanar distances were determined by diffraction program and next crystallographic plane type was defined. The broken Charpy specimens at ambient (25°C) were examined by SEM to study fracture topography of the samples.

## 3. Results of experiments

### 3.1. Dilatometer examinations

Table 2 shows the measurement results of critical transformation temperature for all steels tested. Dilatometer analysis revealed that the start of the austenite transformation temperature $A_{c1}$ was in the range from 709 to 723°C. The finish of austenite transformation temperature $A_{c3}$ was obtained in temperature range from 851 to 878°C. Systematic decrease of the start bainite transformation temperature $B_s$ was observed with increasing concentration of molybdenum. For the samples W1 and W3 were obtained to be 535 and 473°C, respectively. The temperature of the finish bainite transformation $B_f$ was a similar trend. For the samples W1 and W3 were obtained at 362 and 315°C, respectively.

TABLE 2

The average values of phase transformation temperatures

| Steel | $A_{c1}$ | $A_{c3}$ | $B_s$ | $B_f$ |
|---|---|---|---|---|
| | °C | | | |
| W1 | 709 | 851 | 535 | 362 |
| W2 | 727 | 878 | 500 | 349 |
| W3 | 723 | 854 | 473 | 315 |

### 3.2. Mechanical properties

The hardness change after water quenched and tempering of all steels are shown in Fig. 2. The change of hardness as a function of tempering temperature was analyzed in the range of 400 to 800°C. Maximum hardness of all heats was obtained after tempering at 500°C. Highest hardness obtained in the steel W3 with the highest concentration of molybdenum. Decrease of hardness of all heats was observed after tempering above 500°C. The minimum hardness in the temperature range 700-725°C was obtained. The lowest hardness for steel W1 amounting 283 $HV_{30}$ after the process of water quenching was measured, while the highest hardness in the steel W3 equal 315 $HV_{30}$ were observed.

The variation in yield strength (YS), ultimate tensile strength (UTS) and impact toughness after tempering at different temperatures are shown in Fig. 3a-c. These changes of mechanical properties as function of tempering temperature are typical for the steel with the copper addition. The highest strength in all three heats were obtained after water quenching followed by tempering at a temperature of 500°C. Maximum tensile strength corresponds to minimum of notch impact

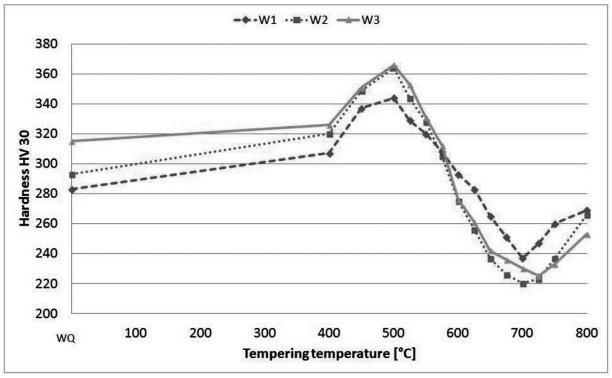


Fig. 2. Mechanical properties of the steels after different tempering temperature, where: WQ – water quenching

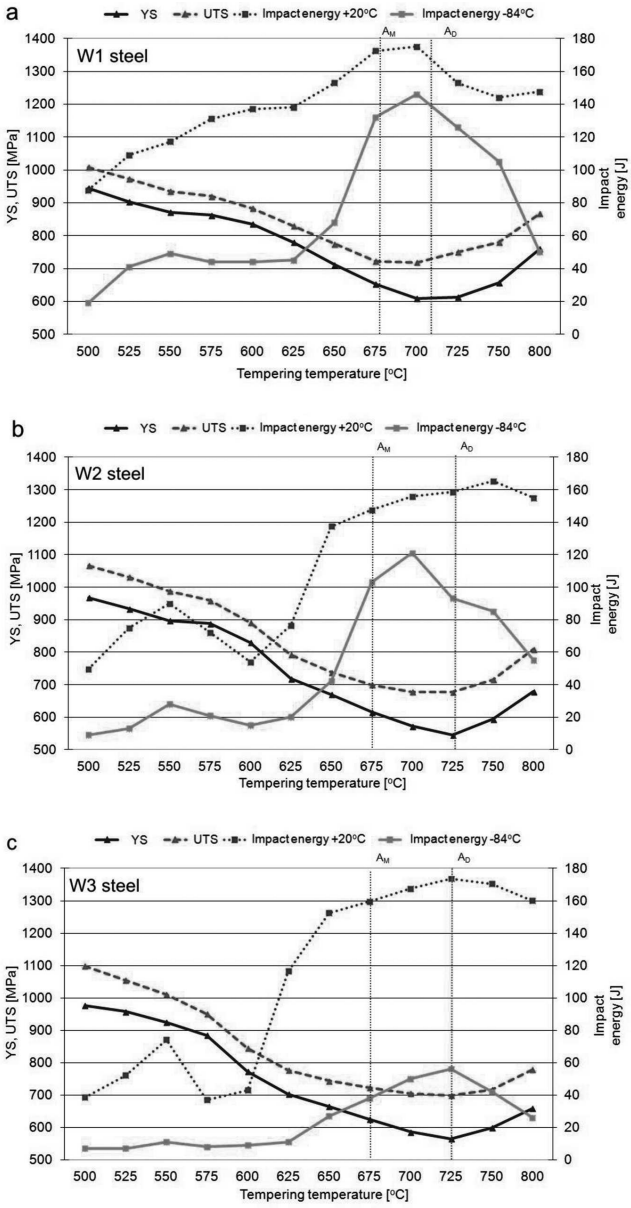


Fig. 3. Results of yield strength, ultimate tensile strength and impact energy at 20°C and -84°C as a function of tempering temperature: a) W1 steel, b) W2 steel, c) W3 steel, where: $A_M$ – ferrite to austenite transformation temperature defined on the basis of microstructure, $A_D$ – ferrite to austenite transformation temperature defined on the basis of dilatometer test

toughness. The YS and UTS of the steel W3 amounted to 977 MPa and 1098 MPa respectively. The Charpy V-notch results at ambient temperature and -84°C were 39 J and 7J properly. The increase in tempering temperature above 500°C caused a decrease in mechanical properties. Minimum strength for all plates were reported for tempering temperatures ranging from 700 to 725°C. Increase in tempering temperature for steel W1 conducted to improve the CVN at ambient temperature and maximum impact toughness was obtained at 700°C.

Tempering of steel W1 in the temperature range from 550 to 625°C conducted to the stabilization of the impact resistance at -84°C, subsequently showed strong growth with a maximum at 700°C. For steels W2 and W3 with a higher amount of molybdenum significantly greater decrease in mechanical properties with a minimum after tempering at 725°C were observed. Different course of CVN at ambient temperature for the higher content of molybdenum was obtained. For steels W2 and W3 characteristic minimum CVN after tempering in the temperature range 575-600°C were observed. The increase of tempering temperature above 600°C caused a sharp increase in impact toughness. The maximum impact strength for all analyzed steels were measured after tempering in the temperature range 700-750°C.

### 3.3. Microstructure

Microscopic observations in unetched conditions revealed that in all steels, non-metallic inclusions were shaped as chains, Fig. 4a-b. Chemical composition analysis by using Energy Dispersive Spectroscopy (EDS) showed that these chains were composed basicly as particles of $Al_2O_3$. Few small elongated MnS type sulphides were also observed in these steels. The quantitative analysis revealed a similar volume fraction of inclusions in W1 and W3 steels. The steel W2 characterized by the higher volume of the inclusions. Results of stereological measurements of non-metallic inclusions are presented in Table 3. Metallographic examination revealed that the average prior austenite grain size for the analyzed heats was about 24 $\mu$m.

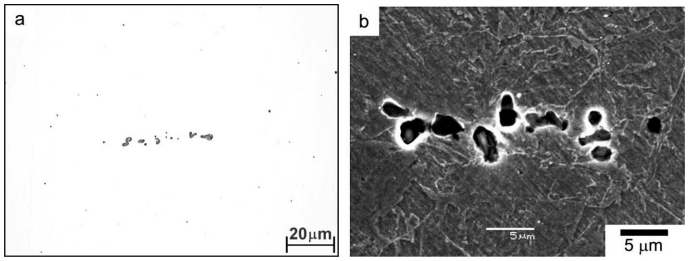


Fig. 4. Micrographs of non-metallic inclusions in W1 steel: a) optical microscopy, b) SEM

The bainitic microstructure of W1 and W3 steels after cooling in the dilatometer is presented in Fig. 5a-b. Bainite morphology obtained after cooling in a dilatometer has not revealed significant differences. SEM and TEM observations of the as water quenched steels revealed microstructures of highly dislocated lath martensite, Fig. 6a-b. SEM observations done for the initial tempering temperature revealed no significant differences in microstructure of the steels. Some changes were observed in transmission electron microscope.

TEM analysis (Fig. 7a-d) of the tempered at 575°C W3 steel revealed mixed microstructure of 200-500 nm wide laths of tempered martensite and areas of polygonal ferrite with very fine particles of $\varepsilon$_Cu. A selected area of diffraction pattern from $\varepsilon$_Cu particles is shown in Fig. 7e. The Cu precipitates observed were around 5-15nm in diameter and were almost spherical in shape. The Cu particles spherical in shape and with a diameter in the range of 5-15 nm is shown in Fig. 7c-d. Furthermore particle size of 50-60 nm at the phase boundaries were observed, Fig. 7f-g. The EDS analysis from this spherical particles showed a high concentration of iron and molybdenum, Fig. 7h. This may suggest occurrence precipitation process of Laves phase $Fe_2Mo$ type. Significant changes of the microstructure by using SEM were observed when $\alpha \rightarrow \gamma$ transformation started at temperature 675°C. Intercritical annealing in the range $(\alpha + \gamma)$ and subsequently cooling the samples in water caused formation of multiphase structure consisting of polygonal ferrite with $\varepsilon$_Cu particles and new formed martensite laths, with a growing volume of martensite. After tempering at 800°C the microstructure consisted of martensite laths with locally occurring bainite regions.

TABLE 3
Average values of stereological parameters of non-metallic inclusions in the steels

| Stereological parameters | Steel | | |
|---|---|---|---|
| | ***W1*** | ***W2*** | ***W3*** |
| $V_v$ [%] | 0,061±0,006 | 0,067±0,007 | 0,061±0,006 |
| $N_A$ [mm$^{-2}$] | 210 ±14 | 275 ±30 | 211 ±18 |
| Σb [$\mu$m/mm$^2$] | 430 ±32 | 534 ±96 | 420 ±38 |
| A±ΔA [$\mu$m$^2$] | 2,93 ±0,06 | 2,36 ±0,26 | 3,08 ±0,31 |

where: $V_v$ – volume fraction, $N_A$ – number of particles per unit test area, Σb – total length of particles per unit test area, A – planar area of particles

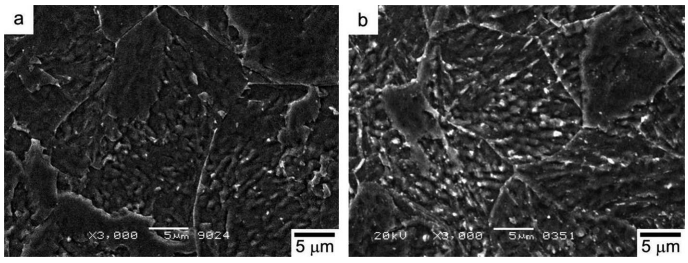


Fig. 5. SEM micrographs of the steels after cooling in the dilatometer: a) W1 steel, b) W 3 steel

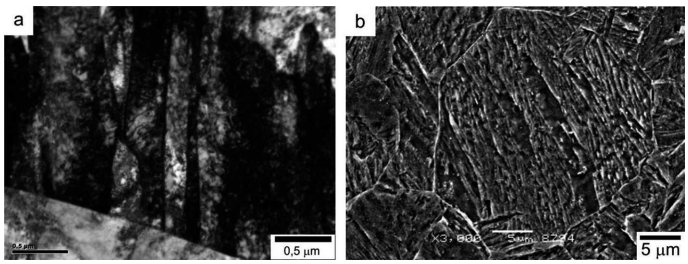


Fig. 6. Microstructure of W3 steel after water quenching: a) TEM, b) SEM

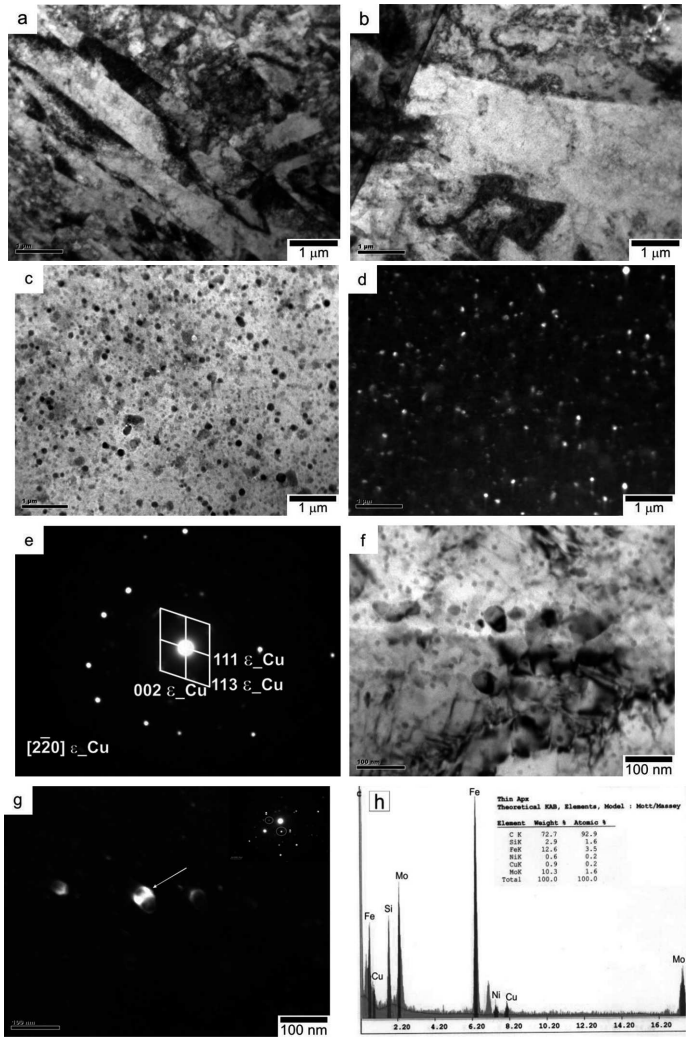


Fig. 7. TEM micrographs of the W3 steel tempered at 575°C: a) recovered martensite lath, b) polygonal ferrite with $\varepsilon$_Cu precipitates, c, d) precipitate of $\varepsilon$_Cu – bright field and dark field, e) SAD pattern and index of SAD pattern identifying of $\varepsilon$_Cu particles, f, g) precipitate of Mo-rich particles (arrow) – bright field and dark field, h) EDS from a Mo-rich particle

### 3.4. Fractography

Typical SEM fractographs of broken Charpy specimens tested at ambient temperature as water quenched as well as tempered (500-750°C) plates of steel W3 are shown in Fig. 8 a-f. After water quenching steel exhibited ductile fracture as a result of the equiaxed microvoids, Fig. 8a. The change in the mechanism of cracking was observed after tempering at 500°C. Generally dominated brittle fracture mechanism with a small area of ductile failure, Fig. 8b. The increase of tempering temperature conducted the growth of ductile fracture surface, Fig. 8c. After tempering at 575°C additional change of cracking mechanism on transcrystalline with a small fraction of ductile and cleavage cracking were observed, Fig. 8d. This way of cracking suggests precipitation of secondary phases at grain boundaries of primary austenite and leads to a drastic reduction of the fracture toughness of the steels. At 625°C improvement in impact toughness values is obtained and the fracture mode has been changed to transgranular cleavage and ductile failure, Fig 8e. Annealing of steel in the temperature

range from 650 to 800°C caused appearance of ductile failure mechanism, Fig. 8f.

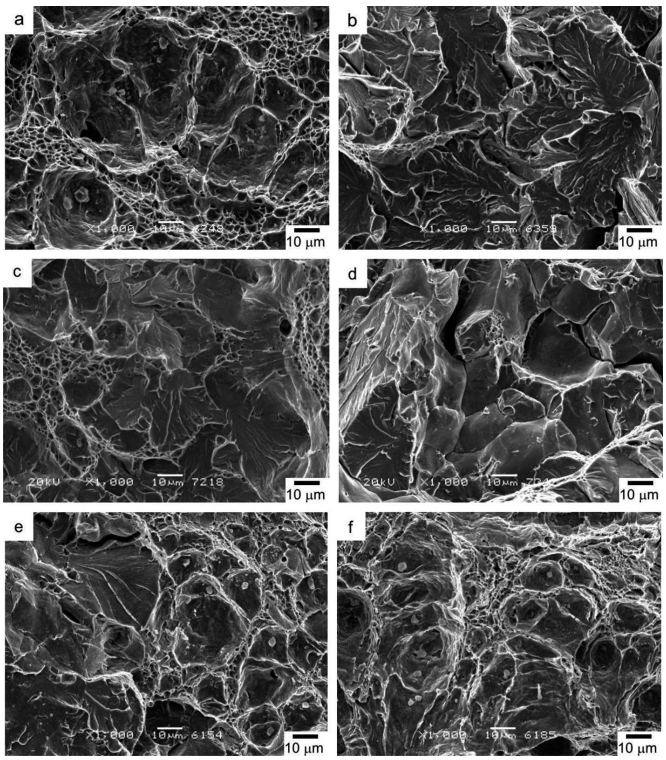


Fig. 8. The variation in fracture surface after tempering at different temperature of broken Charpy specimens at ambient temperature of W3 steel: a) water quenching, b) 500°C, c) 525°C, d) 575°C, e) 625°C, f) 650°C

## 4. Disscusion

The addition of molybdenum does not significantly affect the start and end of the austenite transformation temperature, whereas its effect is significant for the temperature of beginning and end of bainitic transformation. Increase of molybdenum concentration leads to a reduction of bainitic transformation temperature. Yield strength after water quenching increases with growth of molybdenum content which is consistent with earlier research [11-12]. It is associated with a strengthening solution of molybdenum, as suggested in the work [12]. In the case of impact resistance at ambient temperature opposite trend was observed. The highest impact 132 J for steel W1 (1,02% wt. Mo), the lowest 105 J for steel W3 (2,94% wt. Mo) was reported. The observed changes in mechanical properties as a function of tempering temperature exhibit a similar course for all the steels and they are characteristic for the traditional HSLA 100 steel with Cu addition. The increase of YS, UTS and drastic drop of impact resistance after tempering at 500°C is associated with the beginning of the particles $\varepsilon$_Cu precipitation [1,5]. The precipitated particles are *Guinier-Preston* (GP) zones with crystallographic structure which is the same as matrix [1]. The reaction of the dislocations with GP zones consists of a shearing of particles by dislocations in accordance with the Friedel mechanism [19]. As a result, the faults are formed in GP zones which they lead to strengthening of matrix and sudden decrease of the crack resistance [1]. Increase of impact toughness and reduction of mechanical properties during annealing above 500°C are caused of laths martensite decomposition with a coarse of Cu precipitates and decrease their coherence with matrix [1,5]. This was confirmed by fractographic observations. The increase in the share of ductile fracture was observed after tempering in the range from 525 to 550°C, Fig. 8c. The sudden drop in ductility in the range of tempering temperature 575-600°C was connected with a intercrystalline fracture, Fig. 8d. The reason of this phenomenon is probably due to the precipitation of Mo-rich particles at the phase boundaries, Fig. 7f-g. The low carbon concentration of steels suggests that the observed precipitates are probably the Laves phase $Fe_2Mo$. This was confirmed by the TEM analysis of chromium steels with low carbon content and high concentration of Mo which revealed occurrence of Laves phase type $Fe_2Mo$ after annealing in the temperature about 600°C [20-23]. Tempering above 600°C led to sudden increase of impact toughness and a change of cracking mechanism for ductile fracture. It is probably connected with the dissolution of the Laves phase as well as further processes of martensite decomposition and growth of particles $\varepsilon$_Cu. In paper [21] was observed dissolution process of Laves phase above 660°C for steel with 11% chromium and 1,4% molybdenum addition. A sudden increase of impact toughness at ambient temperature is interpreted by presence of a stable retained austenite, whose appearance is associated with the beginning of transformation $\alpha \rightarrow \quad \gamma$ [15]. For all steels tested the maximum value of impact resistance was obtained from 700 to 725°C. This corresponded to the annealing of steel in dual-phase range $\alpha + \gamma$. With the increase of the tempering temperature, volume fraction of retained austenite increases with simultaneous decrease of its thermal stability caused by a reduction of the amount of alloying elements. Annealing in intercritical range $\alpha + \gamma$ with subsequent accelerated cooling caused the formation of martensite laths. As result is sudden decrease of impact energy at temperature of -84°C joined with the increase of YS and UTS. Lower mechanical properties of W2 and W3 steels after tempering above 550°C may be caused by carbide precipitates, as suggested by the results presented in the work [24]. However, this requires further metallographic examination by TEM.

## 5. Conclusions

1. The addition of molybdenum up to 3,0% wt. improves the YS and UTS of low carbon Cu bearing high strength steel after austenitizing at 920°C for one hour followed by a water quench and tempering to 550°C for one hour and water cooled to room temperature.
2. Sudden decrease in ductility in the analyzed steels after tempering in the temperature range 575-600°C are probably associated with precipitates of Laves phase particles of type $Fe_2Mo$ at the grain boundaries.
3. Increase of ductility with simultaneous decrease in strength after tempering above 600°C is the result of decomposition processes of martensitic matrix and growth of $\varepsilon$_Cu precipitates.
4. The maximum ductility was obtained after tempering in the temperature range 700-725°C which corresponds to annealing in the dual-phase range $\alpha + \gamma$.

5. Improvement of the yield strength and tensile strength after tempering above 725°C is due to the increase in the volume fraction of the newly formed of martensite laths.

## REFERENCES

[1] M. Mujahid, A.K. Lis, C.I. Garcia, A.J. De Ardo, Processing, Microstructure and Properties of Microalloyed and Other Modern High Strength Low Alloy Steels, Pittsburgh (1991).
[2] S.J. Mikalac, M.G. Vassilaros, Processing, Microstructure and Properties of Microalloyed and Other Modern High Strength Low Alloy Steels, Pittsburgh (1991).
[3] M. Blicharski, C.I. Garcia, S.M. Pytel, Processing, Microstructure and Properties of HSLA Steels, Pittsburgh, (1987).
[4] R.P. Foley, M.E. Fine, Processing, Microstructure and Properties of Microalloyed and Other Modern High Strength Low Alloy Steels, Pittsburgh (1991).
[5] S.K. Dhua, A. Ray, D.S. Sarma, Mater. Sci. Eng. A **318** (2001).
[6] S. Panwar, D.B. Goel, O.P. Pandy, K.S. Prasad, Bull. Mater. Sci. **26** (2003).
[7] B. Niżnik, M. Pietrzyk, Arch. Metal. Mater. **56** (2011).
[8] S.W. Thompson, Mater. Char. **77** (2013).
[9] S.K. Ghosh, A. Haldar, P.P. Chattopadhyay, Mater. Chem. Phys. **119** (2010).
[10] A. Ghosh, S. Das, S. Chatterjee, Mater. Sci. Eng. A **486** (2008).
[11] W.B. Lee, S.G. Hong, C.G. Park, K.H. Kim, S.H. Park, Scr. Mater. **43** (2000).
[12] K. Junhua, Z. Lin, G. Bin, L. Pinghe, W. Aihua, X. Changsheng, Materials and Design 25 (2004).
[13] A. Ghost, B. Mishra, S. Das, S. Chatterjee, Mater. Sci. Eng. A **396** (2005).
[14] A. Ghost, S. Chatterjee, Mater. Char. **55**, 298-306 (2005).
[15] R. Bogucki, S.M. Pytel, Arch. Metal. Mater. **55** (2010).
[16] S.K. Ghosh, S.K. Sen, Mater. Sci. Eng. A **528** (2011).
[17] S.K. Ghosh, P.S. Bandyopadhyay, S. Kundu, S. Chatterjee, Mater. Sci. Eng. A **528** (2011).
[18] S.K. Ghosh, A. Haldar, P.P. Chattopadhyay, Mater. Char. **59** (2008).
[19] B. Reppich, Mater. Sci. Techn. **6** (1993).
[20] S. Ku, J. Yu, Scr. Mater. **45** (2001).
[21] G. Dimmler, P. Weinert, E. Kozeschnik, H. Cerjak, Mater. Char. **51** (2003).
[22] V. Vodárek, Mater. Sci. Eng. A **528** (2011).
[23] V. Vodárek, Scr. Mater. **66** (2012).
[24] W.B. Lee, S.G. Honh, C.G. Park, K.H. Kim, S.H. Park, Scr. Mater. **43** (2000).

*Received: 10 January 2014.*